Since January 2020 Elsevier has created a COVID-19 resource centre with free information in English and Mandarin on the novel coronavirus COVID-19. The COVID-19 resource centre is hosted on Elsevier Connect, the company's public news and information website.

Journal Pre-proof

Post-acute COVID-19 is characterized by gut viral antigen persistence in inflammatory bowel diseases

Andreas Zollner, Robert Koch, Almina Jukic, Alexandra Pfister, Moritz Meyer, Annika Rössler, Janine Kimpel, Timon E. Adolph, Herbert Tilg

PII: S0016-5085(22)00450-4
DOI: https://doi.org/10.1053/j.gastro.2022.04.037
Reference: YGAST 65033

To appear in: *Gastroenterology*
Accepted Date: 20 April 2022

Please cite this article as: Zollner A, Koch R, Jukic A, Pfister A, Meyer M, Rössler A, Kimpel J, Adolph TE, Tilg H, Post-acute COVID-19 is characterized by gut viral antigen persistence in inflammatory bowel diseases, *Gastroenterology* (2022), doi: https://doi.org/10.1053/j.gastro.2022.04.037.

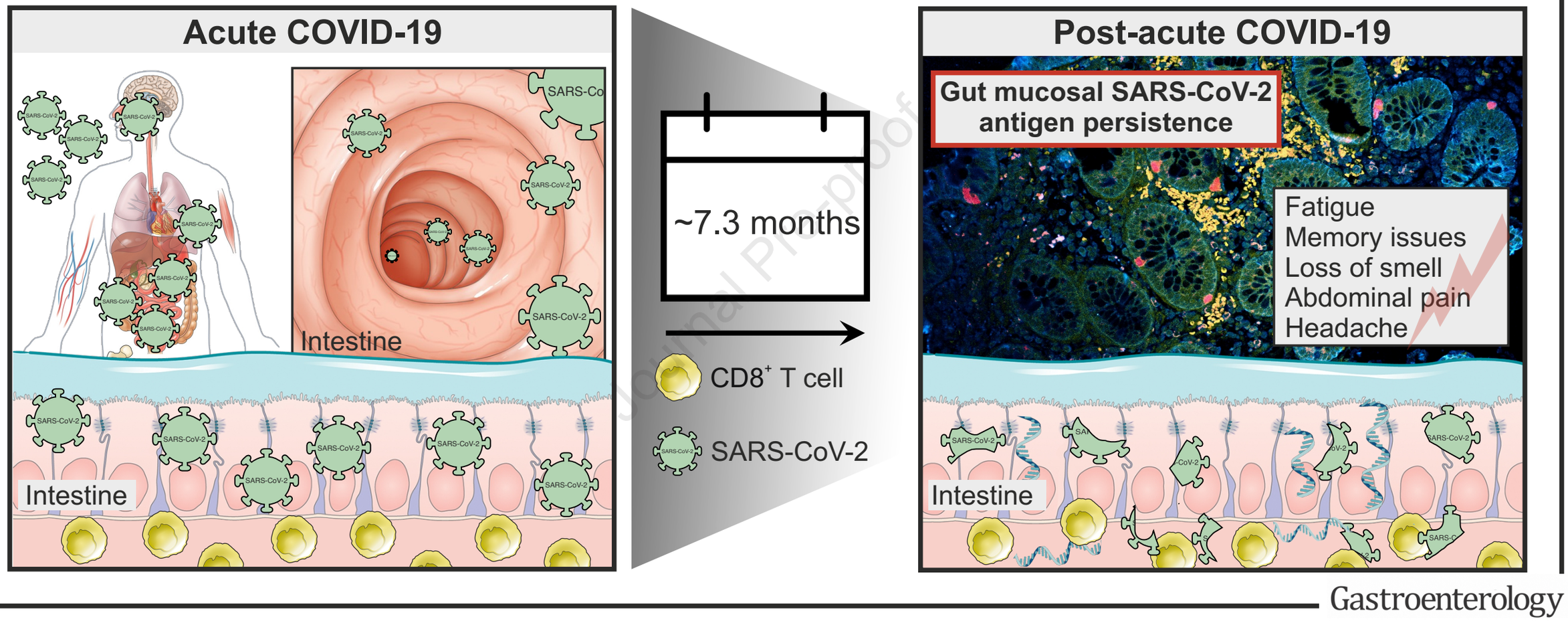

Gastroenterology

Post-acute COVID-19 is characterized by gut viral antigen persistence in inflammatory bowel diseases

Andreas Zollner[1#], Robert Koch[1#], Almina Jukic[1], Alexandra Pfister[1], Moritz Meyer[1], Annika Rössler[2], Janine Kimpel[2], Timon E. Adolph[1*] & Herbert Tilg[1*]

[1] Department of Internal Medicine I, Gastroenterology, Hepatology, Endocrinology & Metabolism, Medical University of Innsbruck, Innsbruck, Austria
[2] Department of Hygiene, Microbiology and Public Health, Institute of Virology, Medical University of Innsbruck, Innsbruck Austria

Authors share co-first authorship

Correspondence to:
Timon E. Adolph, MD, PhD or Herbert Tilg, MD, Department of Internal Medicine I, Gastroenterology, Hepatology, Endocrinology & Metabolism, Medical University of Innsbruck, 6020 Innsbruck, Austria. Email: timon-erik.adolph@i-med.ac.at or herbert.tilg@i-med.ac.at
Phone: +43 (0)512-504-23539, Fax: +43 (0)512-504-23538

Disclosures: The authors have no competing interests to declare.

Grant support: We are grateful for the support from the European Research Council (#101039320) and the Austrian Science Fund (FWF P33070) (to T.E.A). We thank for the financial support from the Excellence Initiative (Competence Centers for Excellent Technologies - COMET) of the Austrian Research Promotion Agency FFG: Research Center of Excellence in Vascular Ageing Tyrol, VASCage (K-Project Nr. 843536) funded by BMVIT, BMWFW, Wirtschaftsagentur Wien and Standortagentur Tirol (to H.T.).

Author contributions: A.Z., R.K., T.E.A. and H.T. designed the study, performed endoscopy and prepared the manuscript. A.J., A.P and M.M. helped with experimentation. A.R. and J.K. performed viral replication analysis.

Data Transparency Statement: Data will be made available after publication

Abstract

Background and aims: The coronavirus disease 2019 (COVID-19) pandemic affects populations, societies and lives for more than two years. Long-term sequelae of COVID-19, collectively termed the post-acute COVID-19 syndrome, are rapidly emerging across the globe. Here, we investigated whether severe acute respiratory syndrome coronavirus 2 (SARS-CoV-2) antigen persistence underlies the post-acute COVID-19 syndrome.

Methods: We performed an endoscopy study with 46 inflammatory bowel disease (IBD) patients 219 days (range: 94-257) after a confirmed COVID-19 infection. SARS-CoV-2 antigen persistence was assessed in the small and large intestine by qPCR of four viral transcripts, immunofluorescence of viral nucleocapsid and virus cultivation from biopsy tissue. Post-acute COVID-19 was assessed by a standardized questionnaire, and a systemic SARS-CoV-2 immune response was evaluated by flow-cytometry and ELISA at endoscopy. IBD activity was evaluated by clinical, biochemical and endoscopic means.

Results: We report expression of SARS-CoV-2 RNA in the gut mucosa ~7 months after mild acute COVID-19 in 32 of 46 patients with IBD. Viral nucleocapsid protein persisted in 24 of 46 patients in gut epithelium and $CD8^+$ T cells. Expression of SARS-CoV-2 antigens was not detectable in stool and viral antigen persistence was unrelated to severity of acute COVID-19, immunosuppressive therapy and gut inflammation. We were unable to culture SARS-CoV-2 from gut tissue of patients with viral antigen persistence. Post-acute sequelae of COVID-19 were reported from the majority of patients with viral antigen persistence, but not from patients without viral antigen persistence.

Conclusion: Our results indicate that SARS-CoV-2 antigen persistence in infected tissues serves as a basis for post-acute COVID-19. The concept that viral antigen persistence instigates immune perturbation and post-acute COVID-19 requires validation in controlled clinical trials.

Keywords: SARS-CoV-2, COVID-19, post-acute COVID-19, viral antigen persistence.

Introduction

Severe acute respiratory syndrome coronavirus 2 (SARS-CoV-2) is a single-stranded positive-sense RNA virus causing respiratory, gastrointestinal, and central nervous system infections in humans collectively referred to as coronavirus disease 2019 (COVID-19).[1] Cellular SARS-CoV-2 infection is mediated by an interaction of membrane-bound angiotensin-converting enzyme 2 (ACE2) with the viral spike and is facilitated by the host proteases TMPRSS2, TMPRSS4 and CatB/L.[2] ACE2 is expressed in the brush border of enterocytes in the gut,[3] a site of SARS-CoV-2 associated inflammation.[4] Studies with intestinal epithelial organoids confirmed that SARS-CoV-2 infects human epithelium, triggering an interferon (IFN)-signature.[5] Consequently, SARS-CoV-2 can be detected in anal swabs, a signal which remains positive long after nasopharyngeal swabs are negative.[6]

The post-acute COVID-19 syndrome is characterised by persistent or prolonged symptoms for more than four weeks after acute COVID-19. Considerable disagreement about definition, and thus prevalence, of post-acute COVID-19 exists, ranging from 10% to 87% of patients with COVID-19.[7, 8] The syndrome was initially dismissed by many but is now recognized as a multi-organ disease, which reflects a significantly growing health care challenge.[9, 10] Post-acute COVID-19 typically involves symptoms including severe fatigue, cognitive dysfunction or pain.[11] Poor baseline health status and severe acute COVID-19 convey risk for the development of post-acute COVID-19, however, also mild COVID-19 (e.g. in non-hospitalised patients) may culminate in post-acute sequelae.[12] Although post-acute COVID-19 symptoms usually do not require hospitalisation,[13] disease burden weighs heavily on affected individuals.[12] While the pathophysiologic mechanisms of acute COVID-19 are well defined (e.g. viral toxicity, microvascular injury, immune dysregulation and inflammation),[1] post-acute COVID-19 sequelae are poorly understood. It appears plausible that viral immune perturbation and/or inflammatory tissue injury during the acute infection account for the post-acute COVID-19 syndrome.[9] For example, neural accumulation of memory T cells in COVID-19 was observed in post-acute COVID-19 neuropsychiatric sequelae (e.g. malaise and depression), and reflects a hallmark of immune senescence during aging and tissue injury.[9] Furthermore it was shown that post-acute COVID-19 was associated with persistently activated innate immune cells and hyperactivated T and B cells, along with increased proinflammatory cytokine expression,[14] while the cause of such prolonged immune perturbation is unknown.

Here, we took advantage of upper and lower gastrointestinal endoscopy (and related mucosal tissue availability) in patients with or without post-acute COVID-19 symptoms who were evaluated in our inflammatory bowel disease outpatient unit, to explore whether gut antigen persistence[15] underlies long-term sequelae of COVID-19.

Methods

Study participants and endoscopy

In a cohort of 46 IBD patients with PCR-confirmed SARS-CoV-2 infection, we phenotyped gut tissue retrieved by upper and lower endoscopy 94-257 days (on average 7.3 months) after infection. A significant proportion of the study participants became infected in the second wave in Austria between October 2020 and February 2021 (possibly reflecting infection with the wildtype, alpha and beta variant: Coronavirus (COVID-19) Cases - Our World in Data). A detailed characterisation of the study population is provided in Tables 1 and 2. All patients underwent endoscopy by clinical means according to IBD guidelines, and provided a negative SARS-CoV-2 PCR test at the day of endoscopic examination. We obtained biopsy specimen from the duodenum, terminal ileum, and colon (Fig 1A). Biopsies were collected in formalin, RNAlater or RPMI supplemented with 10% foetal calf serum (FCS; Sigma, Missouri, US). Tissue samples were further processed using SARS-CoV-2 PCR, immunofluorescence, and viral culture to analyse SARS-CoV-2 antigen persistence. All participants received a routine laboratory test and quantification of faecal calprotectin at endoscopy. Furthermore, we investigated the systemic humoral and cellular SARS-CoV-2 immune responses at time of endoscopy. Additionally, patients completed a questionnaire that recorded symptoms of the acute episode of COVID-19 and post-acute COVID-19 symptoms, similar to COVID-19 vaccination status. This study was approved by the ethics committee of the Medical University Innsbruck [EK-No. 1005/2019] and informed consent was obtained from all study subjects.

SARS-CoV-2 PCR from intestinal biopsies

To decipher SARS-CoV-2 RNA persistence in the gastrointestinal tract we isolated RNA as described previously.[16] In brief, RNAlater (Qiagen, Hilden, Germany) preserved biopsy specimens were homogenised in lysing buffer using a Precellys® 24 Homogenisator and a Precellys Tissue RNA kit (both Bertin, Montigny-le-Bretonneux, France). Lysates were applied on RNAeasy columns (Qiagen, Hilden, Germany) and RNA extraction was carried out according to manufacturer's instructions. Total RNA concentration was quantified at 260 nm right after isolation, using a nanodrop 1000 (Peqlab, Erlangen, Germany). RNA was stored at -80°C. RNA was transcribed to cDNA using an M-MLV reverse transcriptase in combination with hexamer primers (Thermo Fisher Scientific, Waltham, MA). cDNA sequences were amplified by polymerase chain reaction using gene-specific primers in combination with SYBR-green chemistry to detect *RNA polymerase* [RdRP], *nucleocapsid phosphoprotein* [Nucleocapsid], *surface glycoprotein* [Spike] and *envelope protein* RNA. Additionally, β-actin, served as a control to validate isolation and transcription efficiency. SARS-CoV-2 specific primers were validated and extensively analysed by Park et al.[17] and are summarised in Supplementary Table 1.

Immunofluorescence

Intestinal biopsy specimens were collected in RPMI and immediately transferred in cryomolds, covered with OCT embedding medium and immersed in cold isopentane with liquid nitrogen until snap-frozen. Cryomolds were stored at -20°C until cryo-sectioning. For downstream immunofluorescence 4µm cryostat sections were cut from the samples and subsequently stained for SARS-CoV-2 nucleocapsid (#PA5114448, Thermo Scientific, Massachusetts, US), epithelial CK18 (#LS-B11232, LifeSpan Biosciences, WA, US), CD8 (#14-0008-80, Thermo Fisher Scientific, Waltham, MA), or LGR5 (#MA5-25644, Thermo Fisher Scientific, Waltham, MA), according to a standardized immunofluorescence protocol (see supplementary methods). Targets were visualized with secondary fluorophore conjugated antibodies. Images were acquired on a Zeiss Axioobserver Z1 microscope in combination with a LSM700 confocal laser scanning system containing four lasers with 405, 488, 555, and 654 nanometre wavelengths (Zeiss, Oberkochen, Germany).

Virus cultivation

Biopsies stored in RPMI supplemented with 10% FCS at -80°C were homogenized using a Precellys® 24 Homogenisator (Bertin, Montigny-le-Bretonneux, France). After homogenisation the lysate was sterile filtrated and used to infect ACE-2 and TMPRSS2 overexpressing Vero cells[18] (Vero-TMPRSS2/ACE2). Three days after infection, wells were analysed for cytopathic effect (CPE). Samples with absent CPE after two passages were regarded negative for infectious virus. Further details are available in the supplementary section.

Anti-SARS-CoV-2 enzyme linked immunosorbent assays

SARS-CoV-2 spike and nucleocapsid protein specific immunoglobulins were quantified using an anti-SARS-CoV-2 QuantiVac ELISA (IgG) and an anti-SARS-CoV-2-NCP-ELISA (IgG) (both Euroimmun, Luebeck, Germany) according to manufacturer's instructions. Anti-nucleocapsid immunoglobulins are categorically reported as negative, borderline, and positive, and anti-spike receptor binding domain (RBD) antibody concentrations are reported as binding antibody units (BAU)/ml.[19]

Cellular SARS-CoV-2 immunity: Interferon gamma release assays (IGRA) and flow cytometry

The presence of SARS-CoV-2 specific T cells directed against the spike and nucleocapsid proteins were assessed by interferon gamma release assays (IGRA) and validated with intracellular flow cytometry.[20] To specifically stimulate SARS-CoV-2 specific T cells, lithium heparin whole blood or isolated peripheral blood mononuclear cells (PBMC) were co-incubated with peptide pools (Miltenyi Biotech, Bergisch-Gladbach, Germany) consisting of 15-mer

peptides with 11 amino acids overlap covering the entire sequence of the spike glycoprotein (pepS) and the complete sequence of the nucleocapsid phosphoprotein (pepN).

Cellular SARS-CoV-2 immunity was quantitatively analysed by a whole blood spike interferon–γ release assay (IGRA) and nucleocapsid IGRA respectively. Spike and nucleocapsid specific IFN-γ values were analysed by ELISA. SARS-CoV-2 specific T cells were expanded and analysed by intracellular flow cytometry (ICFC) in a subset of patients (n=5 without immunosuppressive therapy and n=5 with anti-TNF therapy). As in the IGRA, T cells were stimulated with pepS or pepN and analysed on a CytoFLEX S flow cytometer (Beckman Coulter, California, US) after combined surface (CD45, CD4, CD8, CD45RO, CD69) and intracellular cytokine staining (IFN–γ, TNFα, IL17A, granzyme B). In the IGRA and ICFC, mock and PMA/Ionomycin treated cells served as negative or positive control, respectively. Both IGRA and ICFC are further described in the supplementary section.

Statistics

Statistical significance was assumed at $p<0.05$ with an unpaired two-tailed Student's t-test, a Mann-Whitney U-test or ANOVA and multiple comparisons were corrected using the Sidak multiple comparison test, where appropriate. Categorical variables were analysed using the Fisher exact test. Analysis was conducted using Prism V9 (Graphpad, San Diego, US) and R version 4.1.0 (R Project for Statistical Computing, Vienna, Austria).

Results

SARS-CoV-2 antigen persistence frequently occurs in the gut mucosa

Patients recruited in this study had acute COVID-19 (PCR-confirmed SARS-CoV-2 infection) 219 days (range: 94-257) prior to endoscopy, which was performed to evaluate disease activity of an established IBD (i.e., we did not select for patients with post-acute COVID-19). At endoscopy, patients were evaluated for post-acute COVID-19 symptoms (by a questionnaire) and viral antigen persistence in the gut. We included 46 patients with characteristics, comorbidities, risk factors and medical history summarised in Table 1, and COVID-19 related clinical and biochemical characteristics shown in Table 2. Briefly, 91% (42/46) of patients had experienced mild acute COVID-19, and 45% (21/46) of patients reported at least one post-acute COVID-19 symptom (Table 2). On the day of endoscopic examination, all patients provided a negative COVID-19 nasal or pharyngeal PCR test and did not display clinical signs of a respiratory infection. Endoscopy revealed that the majority of IBD patients (59%) were in remission. We evaluated viral antigen persistence by analysing biopsies from the small and large intestine with quantitative polymerase chain reaction (qPCR), immunofluorescence and viral culture from gut tissue. Moreover, we evaluated a systemic SARS CoV-2-directed immune response and gut inflammation (indicated by faecal calprotectin; Figure 1A). Notably, 70%

(32/46) of patients displayed a positive qPCR signal in at least one segment of the gut (i.e. duodenum, ileum or colon) (Figure 1B). We detected viral RNA in 31% of biopsies, with expression of the *RNA dependent RNA polymerase* (RdRP) in 13.6% of biopsies, the *surface glycoprotein* (Spike) in 11.4% of biopsies, the *nucleocapsid phosphoprotein* (Nucleocapsid) in 10.6% of biopsies, and the *envelope protein* in 6.1% of biopsies (Figure 1C). Detection by qPCR was unrelated to the intestinal location, the time from COVID-19 diagnosis to endoscopy and IBD activity (Figure 1B and Table 2). SARS-CoV-2 expression was not detectable in stool from patients in this cohort (Supplementary Figure 1).

To confirm long-term viral antigen persistence in the mucosa and to confine the cellular localization in the gut, we performed immunofluorescence of intestinal biopsies targeting the nucleocapsid phosphoprotein. The specificity of the immunofluorescence signal was confirmed in ACE2 and TMPRSS2 overexpressing vero cells infected with SARS-CoV-2 (positive control) and mucosal biopsies collected in 2017, i.e., before the pandemic (negative control; Supplementary Figure 2). In 52% (24/46) of patients from our cohort, we detected immunoreactivity against the viral nucleocapsid phosphoprotein in intestinal epithelial cells and immune cells in the lamina propria in the small and large intestine (Figure 2A and Supplementary Figure 2 and 3). Notably, all patients with a positive nucleocapsid qPCR signal (n=13) also displayed nucleocapsid immunoreactivity in at least one of three analysed gut segments (Figure 2B). In addition, 11 patients who were RdRP, spike, or envelope positive in qPCR (but without a nucleocapsid qPCR signal) displayed nucleocapsid immunoreactivity (Figure 2B and Table 2), indicating a patchy expression pattern as previously reported.[15] Nucleocapsid immunoreactivity specifically localized to epithelial cells (Figure 2A, Supplementary Figure 2 and 3), and possibly stem cells (Supplementary Figure 4), and to a lesser extent to $CD8^+$ T cells in the epithelium and lamina propria (Figure 2C).

These observations led us to explore whether viral antigen persistence in the gut mucosa could be explained by SARS-CoV-2 replication. We homogenised biopsy-derived mucosal tissue from each of the 46 patients and co-cultured the lysate with ACE2 and TMPRSS2 overexpressing vero cells. While this model system showed strong replication of SARS-CoV-2 with lysates from nasal swabs of patients with symptomatic acute COVID-19, intestinal biopsy lysates from our cohort did not show evidence of replication (Supplementary Figure 5). Collectively, these data demonstrated that SARS-CoV-2 viral antigen persistence frequently occurs in the gut mucosa even months after acute COVID-19, but was not detectable in stool and appeared unrelated to viral replication.

SARS-CoV-2 antigen persistence links to post-acute sequelae of COVID-19

In a next step, we hypothesised that gut mucosal SARS-CoV-2 antigen persistence links to post-acute sequelae of COVID-19. We stratified patients into two groups based on a positive SARS-CoV-2 qPCR result along the gut. Patients with a positive qPCR result were compared with patients that displayed no evidence for viral antigen persistence by qPCR. Time from and disease characteristics of acute COVID-19 and IBD were comparable between both groups as shown in Table 1 and 2 and Supplementary Table 2. Notably, only patients who displayed viral RNA expression in the gut reported symptoms compatible with post-acute COVID-19 sequelae (Figure 3A). Patients without evidence for viral antigen persistence in our cohort (n=14) did not display post-acute COVID-19 symptoms (Figure 3A). We confirmed this observation by stratifying patients according to nucleocapsid immunoreactivity assessed by immunofluorescence (rather than qPCR positivity) (Figure 3B). Viral antigen persistence occurred in patients with and without immunosuppressive therapy (i.e. azathioprine, anti-TNF therapy or vedolizumab; Figure 3C), and was unrelated to gut inflammation indicated by faecal calprotectin (Figure 3D and Supplementary Table 2).

Finally, we sought to define potential mechanisms of viral antigen persistence in the intestine.[15] We analysed SARS-CoV-2-associated humoral and cellular immune responses with enzyme-linked immunosorbent assays, interferon gamma release assay (IGRA) and by surface and intracellular flow cytometry (ICFC) of peripheral blood cells (using peptide pools mapping the spike and the nucleocapsid proteins). Blood-derived immune cells from patients with gut antigen persistence exhibited a comparable IFN-γ release upon SARS-CoV-2 nucleocapsid exposure as patients without antigen persistence (Figure 3E). We rather noted that patients with gut viral antigen persistence more frequently lacked evidence of anti-nucleocapsid IgG antibodies (Figure 3F) and that anti-TNF immunosuppressive therapy was associated with impaired inflammatory T cell responses upon nucleocapsid peptide stimulation (Figure 3G and Supplementary Figure 6).

Discussion

SARS-CoV-2 infection causes acute COVID-19, ranging from asymptomatic to severe cases, partly depending on immunocompetency of the host.[21] We rationed that viral antigen persistence may underly post-acute sequelae of COVID-19. Our findings indicate that viral antigens, but not infectious virions, persist in the gut mucosa long beyond mild acute COVID-19 in IBD patients. More specifically, antigen persistence occurs in 52-70% of patients after ~7 months in our IBD cohort (dependent on the definition, i.e. a positive nucleocapsid immunofluorescence in any gut segment, or viral RNA expression of at least one of four viral transcripts in any gut segment determined by qPCR). Viral antigen persistence of the nucleocapsid was detectable in epithelial cells and $CD8^+$ T cells in the gut. Viral antigen

persistence was observed in patients with and without immunosuppressive therapy and was unrelated to severity of acute COVID-19 or gut inflammation in IBD at time of endoscopy. We argue that viral antigen persistence reflects incomplete clearance of SARS-CoV-2 rather than subclinical (latent or persistent) infection, as we were unable to replicate virus from biopsy-derived tissue. In line with this, we usually detected only some (but not all) viral transcripts in biopsies from the same patient. Our experimental data rather suggest that immunosuppressive therapy with or without genetic predisposition (affecting the immune system) may promote incomplete viral clearance.[22] Indeed, we find that some patients exhibit a lack of humoral nucleocapsid IgG antibodies, which is pronounced in those with gut antigen persistence. In line with this notion, a previous report demonstrated immune dysregulation, e.g. a decline of nucleocapsid-specific IFN-γ-producing $CD8^+$ T cells in patients with post-acute COVID-19.[23]

To our knowledge, our study is the largest COVID-19-related gastrointestinal endoscopy study today and the first report that links viral antigen persistence with post-acute COVID-19. In our report, only patients with gut antigen persistence (determined by qPCR) reported post-acute COVID-19 symptoms. In contrast, none of the patients without evidence for antigen persistence in the gut reported symptoms of post-acute COVID-19. This observation strongly argues for a role of viral antigen persistence in post-acute COVID-19 and it appears plausible that SARS-CoV-2 antigen persistence, possibly in infected tissues beyond the gut, could impact host immune responses underlying the post-acute COVID-19 syndrome.[1] This notion is supported by an influenza mouse model, demonstrating that ineffective viral clearance modulates adaptive immune responses and the formation of memory T cells in draining lymph nodes of the lung.[24] Along these lines, a recent report demonstrated that patients who survived COVID-19 pneumonia displayed long-term pulmonary $CD8^+$ T cell alterations (while pulmonary antigen persistence was not explored).[25] Our findings also appear notable in light of the observation that T cell activation is prolonged for six months in COVID-19 when compared with other acute viral infections.[26-28] In addition, a recent study revealed highly activated innate immune cells and persistent activation of T cells in individuals suffering from post-acute COVID-19, while the origin of this hyperactivated state remains obscure.[14]

Limitations of our study are the lack of a replication cohort and direct proof that SARS-CoV-2 antigen persistence affects host immune responses. Moreover, we restricted our studies to IBD patients, as it was initially conceived that this population may be particularly vulnerable to COVID-19 infection (with or without an impact on IBD activity). Our findings could be applicable to patients without IBD, as viral antigen persistence has been reported in the gut 2 months after COVID-19 in patients without IBD or immunosuppression.[15] Whether the reported link between gut viral antigen persistence and post-acute COVID-19 is applicable to patients without IBD warrants controlled clinical trials. Our findings are also consistent with a growing body of evidence showing that COVID-19 does not affect gut inflammation in IBD.[29]

Collectively, we provide evidence for SARS-CoV-2 antigen persistence in the gut as a basis for immune perturbation in post-acute COVID-19. Whether viral antigen persistence (in and beyond the gut) underlies the pathophysiology of post-acute COVID-19 warrants further clinical trials, to tackle this rapidly emerging disorder across the globe.[12]

Figures

Figure 1. SARS-CoV-2 antigen persistence frequently occurs in the gut mucosa.

(*A*) Study design. In a cohort of 46 IBD patients with history of COVID-19, 219 days (range: 94-257) after the first positive PCR test endoscopy was performed and biopsy-derived tissue was phenotyped for SARS-CoV-2 mucosal antigen persistence and IBD activity. Patients were also evaluated for symptoms compatible with post-acute COVID-19 sequelae by a questionnaire. The questionnaire was adapted according to the AWMF Post-Covid/long-Covid S1 guidelines[32], and systemic SARS-CoV-2 directed immune responses were analysed. (*B*) SARS-CoV-2 RNA was detected in 32/46 patients by qPCR. Viral RNA was detected in one biopsy in 19 patients, in two biopsies in 9 patients, and in all three biopsies collected in 4 patients. Detection was unrelated to the intestinal location and viral RNA was detected in 15/46 duodenal, 10/46 ileal, and 13/46 colonic samples. (*C*) Biopsies were analysed for four viral transcripts by qPCR (i.e. *RNA polymerase* [RdRP], *nucleocapsid phosphoprotein* [Nucleocapsid], *surface glycoprotein* [Spike] and *envelope protein*). The red bar (left) indicates the proportion of biopsies with at least one positive qPCR signal, the blue bars illustrate the proportions for the respective transcript.

Figure 2. SARS-CoV-2 nucleocapsid immunofluorescence in the intestine

(A) Representative confocal microscopy images of viral nucleocapsid (red) in the duodenum, ileum and colon from IBD patients ~219 days after acute COVID-19. Cytokeratin 18 (blue) visualises the epithelial cytoskeleton and DAPI (yellow) depicts the nucleus. Scale bar indicates 50 µm. (*B*) Association between viral qPCR positivity and anti-nucleocapsid immunoreactivity by immunofluorescence. SARS-CoV-2 RNA was detected in 32/46 patients with *RNA dependent RNA polymerase* (RdRP) in 16 patients, the *surface glycoprotein* (Spike) in 12 patients, the *nucleocapsid phosphoprotein* (Nucleocapsid) in 13 patients, and the *envelope protein* in 7 patients. All patients with a positive nucleocapsid qPCR displayed nucleocapsid immunoreactivity by immunofluorescence in at least one of three gut segments. *(C*) Representative confocal microscopy images of viral nucleocapsid (red) co-labelled with anti-CD8 (blue) in the duodenum, ileum and colon. Cytokeratin 18 (yellow) visualises the cytoskeleton and DAPI (grey) depicts the nucleus. Scale bar indicates 50 µm.

Figure 3. SARS-CoV-2 antigen persistence links to post-acute sequelae of COVID-19.
(*A*) Patients were stratified based on viral qPCR positivity in any gut segment. Patients without evident mucosal viral RNA by PCR (neg.) were compared with patients with detectable viral RNA (pos.). Proportion of patients who reported symptoms compatible with post-acute COVID-19 syndrome is shown in red. Note that 0/14 patients without detectable mucosal viral RNA (by qPCR in any gut segment) reported symptoms, while post-acute COVID-19 symptoms were reported from 21/32 patients with detectable RNA (with specific symptoms listed). Statistical significance was calculated using the Fisher exact test. (*B*) Patients where stratified according to nucleocapsid immunoreactivity as assessed by immunofluorescence and data is depicted equivalent to (A). (*C*) Proportion of patients without IBD medication, with 5-aminosalycilates, and with immunosuppressive therapy (i.e. azathioprine, anti-TNF therapy, or vedolizumab) in both groups (defined by qPCR positivity). (*D*) Quantification of faecal calprotectin concentrations in both groups (defined by qPCR positivity) by ELISA. (E) Quantification of SARS-CoV-2 nucleocapsid specific T cell responses defined by interferon-gamma release (IGRA) (according to qPCR positivity). (*F*) Proportion of patients with positive, borderline, and negative nucleocapsid IgG in both groups (defined by qPCR positivity). Borderline and negative results were pooled, and statistical significance was calculated using the Fisher exact test. (*G*) Relative quantification of indicated cytokines defined by intracellular flow cytometry of T cells from patients with or without anti-TNF therapy after exposure to peptides of the SARS-CoV-2 nucleocapsid (n=5). Boxplots represent median percentages of cytokine positive $CD4^+$ and $CD8^+$ cells. Differences between groups were calculated by the Fisher exact test (A and B), Two-tailed Student's t-tests (D, E and F), and two-way analysis of variance (ANOVA) with Sidak multiple comparison post-hoc test (G).
Boxplots represent values as median [bold horizontal line], interquartile range [box], and 1.5 x IQR [whiskers]. Bars represent the mean and whiskers the standard deviation.

References

1. **Gupta A,** Madhavan MV, Sehgal K, et al. Extrapulmonary manifestations of COVID-19. Nature Medicine 2020;26:1017-1032.
2. **Jackson CB**, Farzan M, Chen B, et al. Mechanisms of SARS-CoV-2 entry into cells. Nature Reviews Molecular Cell Biology 2021.
3. **Penninger JM**, Grant MB, Sung JJY. The Role of Angiotensin Converting Enzyme 2 in Modulating Gut Microbiota, Intestinal Inflammation, and Coronavirus Infection. Gastroenterology 2021;160:39-46.
4. **Effenberger M**, Grabherr F, Mayr L, et al. Faecal calprotectin indicates intestinal inflammation in COVID-19. Gut 2020;69:1543.
5. **Lamers Mart M**, Beumer J, van der Vaart J, et al. SARS-CoV-2 productively infects human gut enterocytes. Science 2020;369:50-54.
6. **Wu Y**, Guo C, Tang L, et al. Prolonged presence of SARS-CoV-2 viral RNA in faecal samples. Lancet Gastroenterol Hepatol 2020;5:434-435.
7. **Carfì A**, Bernabei R, Landi F, et al. Persistent Symptoms in Patients After Acute COVID-19. JAMA 2020;324:603-605.
8. **Greenhalgh T**, Knight M, A'Court C, et al. Management of post-acute covid-19 in primary care. BMJ 2020;370:m3026.
9. **Nalbandian A**, Sehgal K, Gupta A, et al. Post-acute COVID-19 syndrome. Nature Medicine 2021;27:601-615.
10. **Datta SD**, Talwar A, Lee JT. A Proposed Framework and Timeline of the Spectrum of Disease Due to SARS-CoV-2 Infection: Illness Beyond Acute Infection and Public Health Implications. JAMA 2020;324:2251-2252.
11. **Al-Aly Z**, Xie Y, Bowe B. High-dimensional characterization of post-acute sequelae of COVID-19. Nature 2021;594:259-264.
12. **Xie Y**, Bowe B, Al-Aly Z. Burdens of post-acute sequelae of COVID-19 by severity of acute infection, demographics and health status. Nature Communications 2021;12:6571.
13. **Lund LC**, Hallas J, Nielsen H, et al. Post-acute effects of SARS-CoV-2 infection in individuals not requiring hospital admission: a Danish population-based cohort study. Lancet Infect Dis 2021;21:1373-1382.
14. **Phetsouphanh C**, Darley DR, Wilson DB, et al. Immunological dysfunction persists for 8 months following initial mild-to-moderate SARS-CoV-2 infection. Nature Immunology 2022.
15. **Gaebler C**, Wang Z, Lorenzi JCC, et al. Evolution of antibody immunity to SARS-CoV-2. Nature 2021;591:639-644.
16. **Zollner A, Schmiderer A, Reider SJ**, et al. Faecal Biomarkers in Inflammatory Bowel Diseases: Calprotectin Versus Lipocalin-2-a Comparative Study. J Crohns Colitis 2021;15:43-54.
17. **Park M**, Won J, Choi BY, et al. Optimization of primer sets and detection protocols for SARS-CoV-2 of coronavirus disease 2019 (COVID-19) using PCR and real-time PCR. Experimental & Molecular Medicine 2020;52:963-977.
18. **Riepler L**, Rössler A, Falch A, et al. Comparison of Four SARS-CoV-2 Neutralization Assays. Vaccines (Basel) 2020;9.
19. **Kristiansen PA**, Page M, Bernasconi V, et al. WHO International Standard for anti-SARS-CoV-2 immunoglobulin. Lancet (London, England) 2021;397:1347-1348.
20. **Zollner A**, Watschinger C, Rössler A, et al. B and T cell response to SARS-CoV-2 vaccination in health care professionals with and without previous COVID-19. EBioMedicine 2021;70:103539.
21. **Hu B**, Guo H, Zhou P, et al. Characteristics of SARS-CoV-2 and COVID-19. Nature Reviews Microbiology 2021;19:141-154.
22. **McGonagle D**, Kearney MF, O'Regan A, et al. Therapeutic implications of ongoing alveolar viral replication in COVID-19. The Lancet Rheumatology 2021.

23. **Peluso MJ**, Deitchman AN, Torres L, et al. Long-term SARS-CoV-2-specific immune and inflammatory responses in individuals recovering from COVID-19 with and without post-acute symptoms. Cell Rep 2021;36:109518.
24. **Kim TS**, Hufford MM, Sun J, et al. Antigen persistence and the control of local T cell memory by migrant respiratory dendritic cells after acute virus infection. The Journal of experimental medicine 2010;207:1161-1172.
25. **Cheon IS**, Li C, Son YM, et al. Immune signatures underlying post-acute COVID-19 lung sequelae. Sci Immunol 2021;6:eabk1741.
26. **Mathew D, Giles Josephine R, Baxter Amy E**, et al. Deep immune profiling of COVID-19 patients reveals distinct immunotypes with therapeutic implications. Science 2020;369:eabc8511.
27. **Roukens AHE**, Pothast CR, König M, et al. Prolonged activation of nasal immune cell populations and development of tissue-resident SARS-CoV-2-specific CD8+ T cell responses following COVID-19. Nature Immunology 2022;23:23-32.
28. **Ryan FJ**, Hope CM, Masavuli MG, et al. Long-term perturbation of the peripheral immune system months after SARS-CoV-2 infection. BMC Medicine 2022;20:26.
29. **Lukin DJ**, Funez-dePagnier G, Lima S, et al. No Durable Impact of COVID-19 on Intestinal Disease Activity in Subjects With IBD. Clinical Gastroenterology and Hepatology 2021;19:2312-2314.e3.
30. **Satsangi J**, Silverberg MS, Vermeire S, et al. The Montreal classification of inflammatory bowel disease: controversies, consensus, and implications. Gut 2006;55:749-53.
31. WHO Working Group on the Clinical Characterisation and Management of COVID-19 infectin, A minimal common outcome measure set for COVID-19 clinical research. Lancet Infect Dis 2020;20:e192-e197.
32. **Koczulla AR**, Ankermann T, Behrends U, et al. [S1 Guideline Post-COVID/Long-COVID]. Pneumologie 2021;75:869-900.

*Author names in bold designate shared co-first authorship

Tables

Table 1: General characteristics of the study population at recruitment

	Mucosal SARS-CoV-2 RNA negative	Mucosal SARS-CoV-2 RNA positive	Overall	p
n	14	32	46	
Sex				0.36
Female	8/14 (57.1 %)	12/32 (37.5%)	20/46 (43.5 %)	
Male	6/14 (42.9 %)	20/32 (62.5%)	26/46 (56.5 %)	
Disease				0.52
Crohn's disease	9/14 (64.3 %)	22/32 (68.8 %)	31/46 (67.4 %)	
Ulcerative colitis	5/14 (35.7 %)	8/32 (25.0 %)	13/46 (28.3 %)	
IBD unclassified	0/14 (0.0 %)	2/32 (6.2 %)	2/46 (4.3 %)	
Metrics				
Age (years)	45.28 [40.93, 54.48]	44.67 [25.45, 50.58]	44.67 [28.11, 51.95]	0.21
Age at IBD diagnosis (years)	11.05 [6.84, 14.28]	8.60 [4.99, 20.84]	9.92 [5.30, 17.38]	0,75
Duration of IBD (years)	35.51 [28.21, 43.57]	24.96 [17.80, 37.00]	28.60 [18.49, 40.60]	0,02
IBD severity [a]				0.13
Remission	7/14 (50.0 %)	20/32 (62.5 %)	27/46 (58.7 %)	
Mild	4/14 (28.6 %)	11/32 (34.4 %)	15/46 (32.6 %)	
Moderate	3/14 (21.4 %)	1/32 (3.1 %)	4/46 (8.7 %)	
Severe	0/14 (0.0 %)	0/32 (0.0 %)	0/46 (0.0 %)	
Crohn's disease: Age At diagnose [Montreal A] [b]				0.17
<16 years [A1]	0/9 (0.0 %)	6/22 (27.3 %)	6/31 (19.4 %)	
17-40 years [A2]	7/9 (77.8 %)	14/22 (63.6 %)	21/31 (67.7 %)	
>40 years [A3]	2/9 (22.2 %)	2/22 (9.1 %)	4/31 (12.9 %)	
Crohn's disease: Behaviour [Montreal B] [b]				0.37
Non-constricting &n-penetrating [B1]	6/9 (66.7 %)	13/22 (59.1 %)	19/31 (61.3 %)	
Stricturing [B2]	1/9 (11.1 %)	7/22 (31.8 %)	8/31 (25.8 %)	
Penetrating [B3]	2/9 (22.2 %)	2/22 (9.1 %)	4/31 (12.9 %)	
Crohn's disease: Disease Location [Montreal L] [b]				0.25
Ileum [L1]	1/9 (11.1 %)	6/22 (30.0 %)	7/31 (22.6 %)	
Colon [L2]	2/9 (22.2 %)	1/22 (5.0 %)	3/31 (9.7 %)	
Ileum + colon [L3]	6/9 (66.7 %)	15/22 (68.2 %)	21/31 (67.7 %)	
Upper GI [L4]	0/9 (0.0 %)	0/15 (0.0 %)	0/31 (0.0 %)	
Ulcerative colitis: Age at diagnose [Montreal A] [b]				0.46
<16 years [A1]	0/5 (0.0 %)	1/8 (14.3 %)	1/13 (7.7 %)	
17-40 years [A2]	3/5 (60.0 %)	5/8 (71.4 %)	8/13 (61.5 %)	
> 40 years [A3]	2/5 (40.0 %)	1/8 (14.3 %)	3/13 (23.1 %)	
Ulcerative colitis: Disease extent [Montreal E] [b]				0.50
Proctitis [E1]	0/5 (0.0 %)	0/8 (0.0 %)	0/13 (0.0 %)	
Left-sided-colitis [E2]	2/5 (40.0 %)	6/8 (75.0 %)	8/13 (61.5 %)	
Pancolitis [E3]	3/5 (60.0 %)	2/8 (25.0 %)	5/13 (38.5 %)	
Risk factors and other diseases				
BMI	26.20 [21.80, 31.80]	24.50 [22.25, 26.80]	24.95 [22.20, 28.10]	0.31
Smoker	3/14 (21.4 %)	8/32 (25.0 %)	11/46 (23.9 %)	0.99
Abnormality in chest x-ray	4/14 (33.3 %)	7/32 (24.1 %)	11/46 (26.8 %)	0.83
Heart disease	0/14 (0.0 %)	2/32 (6.2 %)	2/46 (4.3 %)	0.86
Diabetes	1/14 (7.1 %)	2/32 (6.2 %)	3/46 (6.5 %)	0.99
Lung disease	1/14 (7.1 %)	1/32 (3.1 %)	2/46 (4.3 %)	0.99
Kidney disease	0/14 (0.0 %)	0/32 (100.0 %)	0/46 (100.0 %)	NA
Medication				
Steroid use in last year	1/14 (7.1 %)	1/32 (3.1 %)	2/46 (4.3 %)	0.99
Anti-TNF at endoscopy	2/14 (14.3 %)	12/32 (37.5 %)	14/46 (30.4 %)	0.22
Ustekinumab at endoscopy	1/14 (7.1 %)	1/32 (3.1 %)	2/46 (4.3 %)	0.99
Vedolizumab at endoscopy	1/14 (7.1 %)	2/32 (6.2 %)	3/46 (6.5 %)	0.99
Azathioprine at endoscopy	0/14 (0.0 %)	4/32 (12.5 %)	4/46 (8.7 %)	0.41
JAK-inhibitor at endoscopy	1/14 (7.1 %)	0/32 (0.0 %)	1/46 (2.2 %)	0.67
5-ASA at endoscopy	4/14 (28.6 %)	5/32 (15.6 %)	9/46 (19.6 %)	0.53
Study medication at endoscopy	2/14 (14.3 %)	0/32 (0.0 %)	2/46 (4.3 %)	0.03
Medication History				
History of anti-TNF	6/14 (42.9 %)	5/32 (15.6 %)	11/46 (23.9 %)	0.11
History of Vedolizumab	3/14 (21.4 %)	1/32 (3.1 %)	4/46 (8.7 %)	0.15
History of Ustekinumab	2/14 (14.3 %)	0/32 (0.0 %)	2/46 (4.3 %)	0.16
History of Azathioprine	6/14 (42.9 %)	9/32 (28.1 %)	15/46 (32.6 %)	0.53
History of JAK-inhibitor	1/14 (7.1 %)	0/32 (0.0 %)	1/46 (2.2 %)	0.67

[a] IBD disease activity was assessed according to the simple endoscopic score for Crohn's disease and the Mayo Endoscopic Score for Ulcerative colitis
[b] Assessment of disease extent, disease location, and disease behaviour by using the Montreal classification[30]
Data are reported as number of subjects with percentages in brackets or as median with interquartile range in brackets
5-ASA=5-aminosalicylic acid; IBD=inflammatory bowel disease; JAK=Januskinase; TNF=tumour necrosis factor

Table 2: SARS-CoV-2 specific characteristics of the study population

	Mucosal SARS-CoV-2 RNA negative	Mucosal SARS-CoV-2 RNA positive	Overall	p
n	14	32	46	
Metrics				
Days between COVID-19 and biopsy sampling	122.00 [72.75, 236.25]	229.50 [107.25, 263.00]	218.50 [94.50, 256.75]	0.17
Lung capacity				
FVC (z-score)	-0.55 [-1.17, 0.55]	-0.64 [-1.08, -0.08]	-0.63 [-1.14, 0.32]	0.97
FEV1 (z-score)	0.54 [-0.44, 0.92]	-0.64 [-1.38, -0.03]	-0.41 [-1.17, 0.57]	0.04
COVID-19 Severity [a]				0.36
Asymptomatic	0/14 (0.0 %)	1/32 (3.1 %)	1/46 (2.2 %)	
Ambulatory: mild disease	12/14 (85.7 %)	30/32 (93.8 %)	42/46 (91.3 %)	
Hospitalised: moderate disease	1/14 (7.1 %)	1/32 (3.1 %)	2/46 (4.3 %)	
Hospitalised: severe disease	1/14 (7.1 %)	0/32 (0.0 %)	1/46 (2.2 %)	
Post-acute COVID-19 symptoms [d]				
Any post-acute COVID symptom	0/14 (0.0 %)	21/32 (65.6 %)	21/46 (45.7 %)	0.001
Fatigue	0/14 (0.0 %)	18/32 (56.3 %)	18/46 (39.1 %)	
Memory issues	0/14 (0.0 %)	14/32 (43.8 %)	14/46 (30.4 %)	
Loss of smell	0/14 (0.0 %)	11/32 (34.4 %)	11/46 (23.9 %)	
Abdominal pain	0/14 (0.0 %)	10/32 (28.1 %)	10/46 (21.7 %)	
Headache	0/14 (0.0 %)	9/32 (28.1 %)	9/46 (19.6 %)	
Sleeping disorders	0/14 (0.0 %)	8/32 (25.0 %)	8/46 (17.4 %)	
Diarrhoea	0/14 (0.0 %)	7/32 (21.9 %)	7/46 (15.2 %)	
Persistent cough	0/14 (0.0 %)	7/32 (21.9 %)	7/46 (15.2 %)	
Shortness of breath	0/14 (0.0 %)	6/32 (18.8 %)	6/46 (13.0 %)	
Depression	0/14 (0.0 %)	3/32 (9.4 %)	3/46 (6.5 %)	
Palpitations	0/14 (0.0 %)	2/32 (6.3 %)	2/46 (4.3 %)	
Muscle pain	0/14 (0.0 %)	2/32 (6.3 %)	2/46 (4.3 %)	
Chest pain	0/14 (0.0 %)	1/32 (3.1 %)	1/46 (2.2 %)	
Rash	0/14 (0.0 %)	0/32 (0.0 %)	0/46 (0.0 %)	
Recurrent fever	0/14 (0.0 %)	0/32 (0.0 %)	0/46 (0.0 %)	
SARS-CoV-2 vaccination status				
Unvaccinated	9/14 (64.3 %)	10/32 (31.2 %)	19/46 (41.3 %)	0.08
One dose Vaxzevria (ChAdOx1)	0/14 (0.0 %)	1/32 (3.1 %)	1/46 (2.2 %)	
One dose Janssen COVID-19 Vaccine	0/14 (0.0 %)	1/32 (3.1 %)	1/46 (2.2 %)	
One dose Comirnaty (BNT162b2)	0/14 (0.0 %)	5/32 (15.6 %)	5/46 (10.9 %)	
Two doses Vaxzevria (ChAdOx1)	0/14 (0.0 %)	1/32 (3.1 %)	1/46 (2.2 %)	
Two doses Spikevax (mRNA-1273)	1/14 (7.1 %)	6/32 (18.8 %)	7/46 (15.2 %)	
Two doses Comirnaty (BNT162b2)	2/14 (14.3 %)	6/32 (18.8 %)	8/46 (17.4 %)	
Three doses Comirnaty (BNT162b2)	2/14 (14.3 %)	2/32 (6.2 %)	4/46 (8.7 %)	
Positive PCR in medical history	14/14 (100 %)	32/32 (100.0 %)	46/46 (100.0 %)	0.99
Anti-Nucleocapsid antibodies				0.18
Negative	1/14 (7.1 %)	3/32 (9.4 %)	4/46 (8.7 %)	
Borderline	1/14 (7.1 %)	10/32 (31.2 %)	11/46 (23.9 %)	
Positive	12/14 (85.7 %)	19/32 (59.4 %)	31/46 (67.4 %)	
Anti-RBD antibodies				0.99
Negative	0/10 (0.0 %)	0/32 (0.0 %)	0/46 (0.0 %)	
Borderline	0/10 (0.0 %)	0/32 (0.0 %)	0/46 (0.0 %)	
Positive	14/14 (100.0 %)	32/32 (100.0 %)	46/46 (100.0 %)	
Nucleocapsid specific T cells (Nucleocapsid IGRA)				0.75
Negative	6/14 (42.9 %)	17/32 (53.1 %)	23/46 (50.0 %)	
Positive	8/14 (57.1 %)	15/32 (46.9 %)	23/46 (50.0 %)	
Spike specific T cells (Nucleocapsid IGRA)				0.99
Negative	3/14 (21.4 %)	7/14 (21.9 %)	10/46 (21.7 %)	
Positive	11/14 (78.6 %)	25/14 (78.1 %)	36/46 (78.3 %)	
Quantitative SARS-CoV-2 immunity				
Anti-RBD antibodies (BAU/ml)	274.60 [43.60, 2053.10]	809.90 [203.65, 1862.60]	658.45 [171.43, 2060.15]	0.32
Spike-IGRA (pg/ml)	1329.05 [60.22, 2018.88]	1922.99 [299.61, 3633.77]	1707.19 [239.56, 3293.65]	0.31
Nucleocapsid-IGRA (pg/ml)	45.79 [3.28, 170.75]	23.65 [0.10, 618.01]	40.38 [0.10, 455.96]	0.96
Nucleocapsid immunofluorescence signal				0.001
Negative	14/14 (100.0 %)	8/32 (25 %)	22/46 (47.8 %)	
Positive	0/14 (0.0 %)	24/32 (75.0 %)	24/46 (52.2 %)	

[a] COVID-19 severity was stratified according to the WHO COVID-19 clinical progression scale[31] and defined as follows: *Mild*; ambulatory and oxygen saturation always >90%. *Moderate*; hospitalisation and/or decrease in oxygen saturation below 90%, but no oxygen supply necessary. *Severe*; hospitalised and oxygen supplementation or high-flow oxygen or intubation

Data are reported as number of subjects with percentages in brackets or as median with interquartile range in brackets

IGRA=interferon gamma release assay; RBD=Receptor binding domain

A

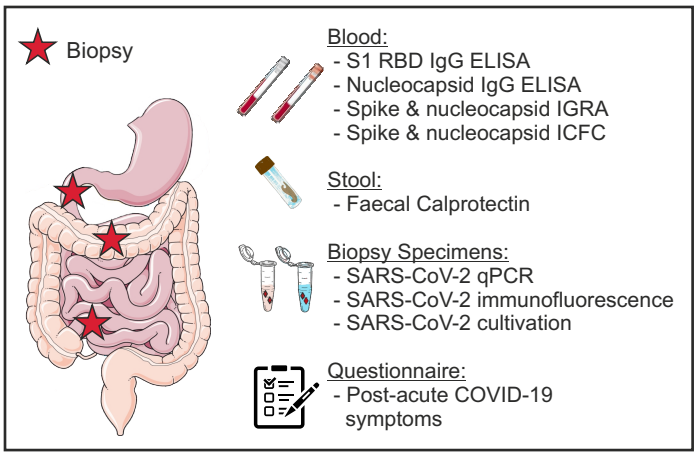

B

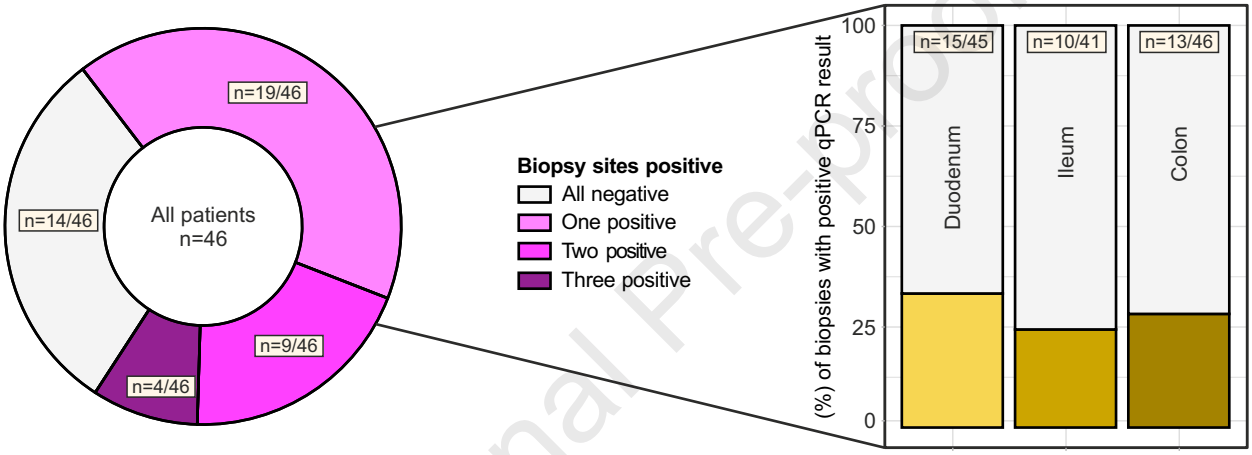

C

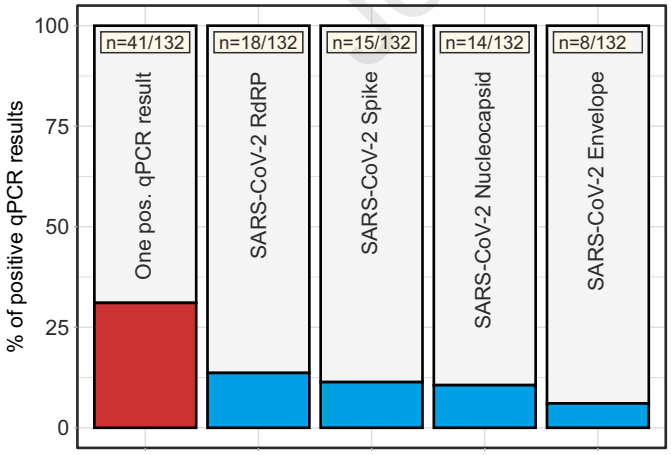

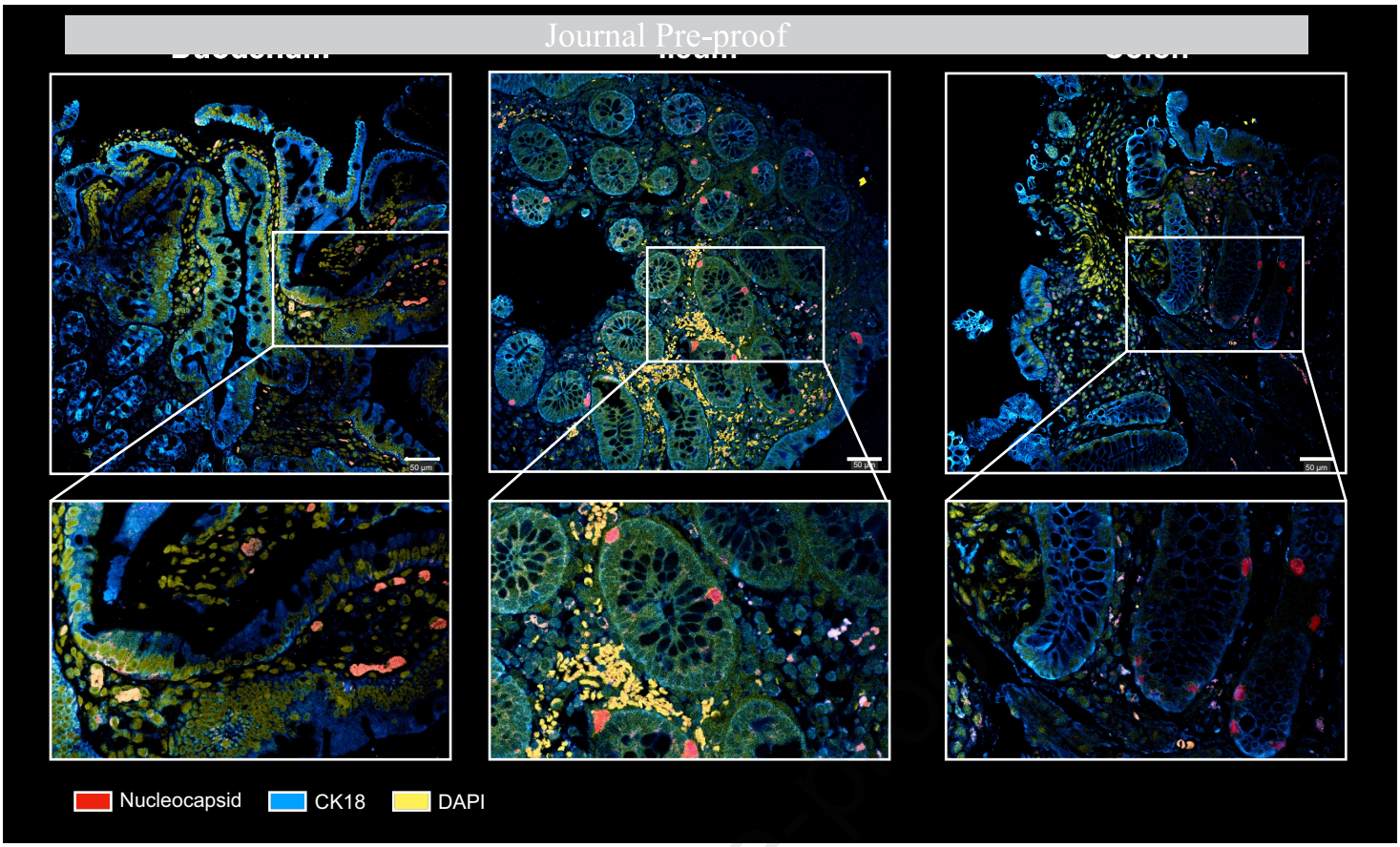

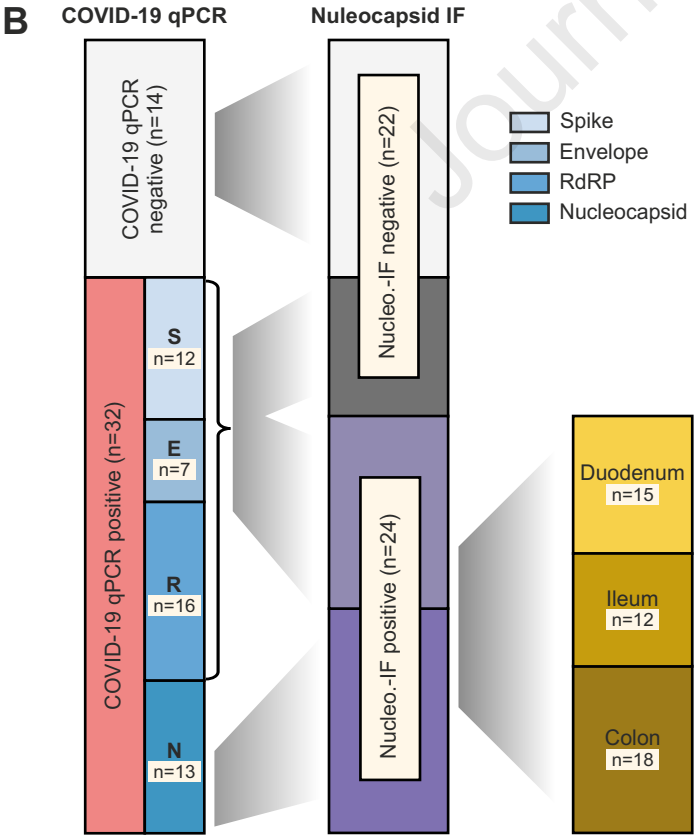

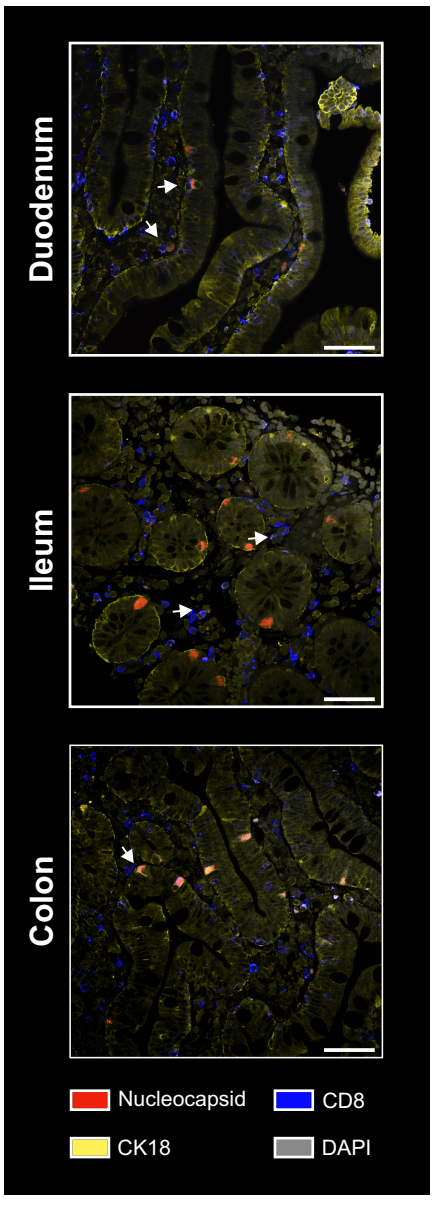

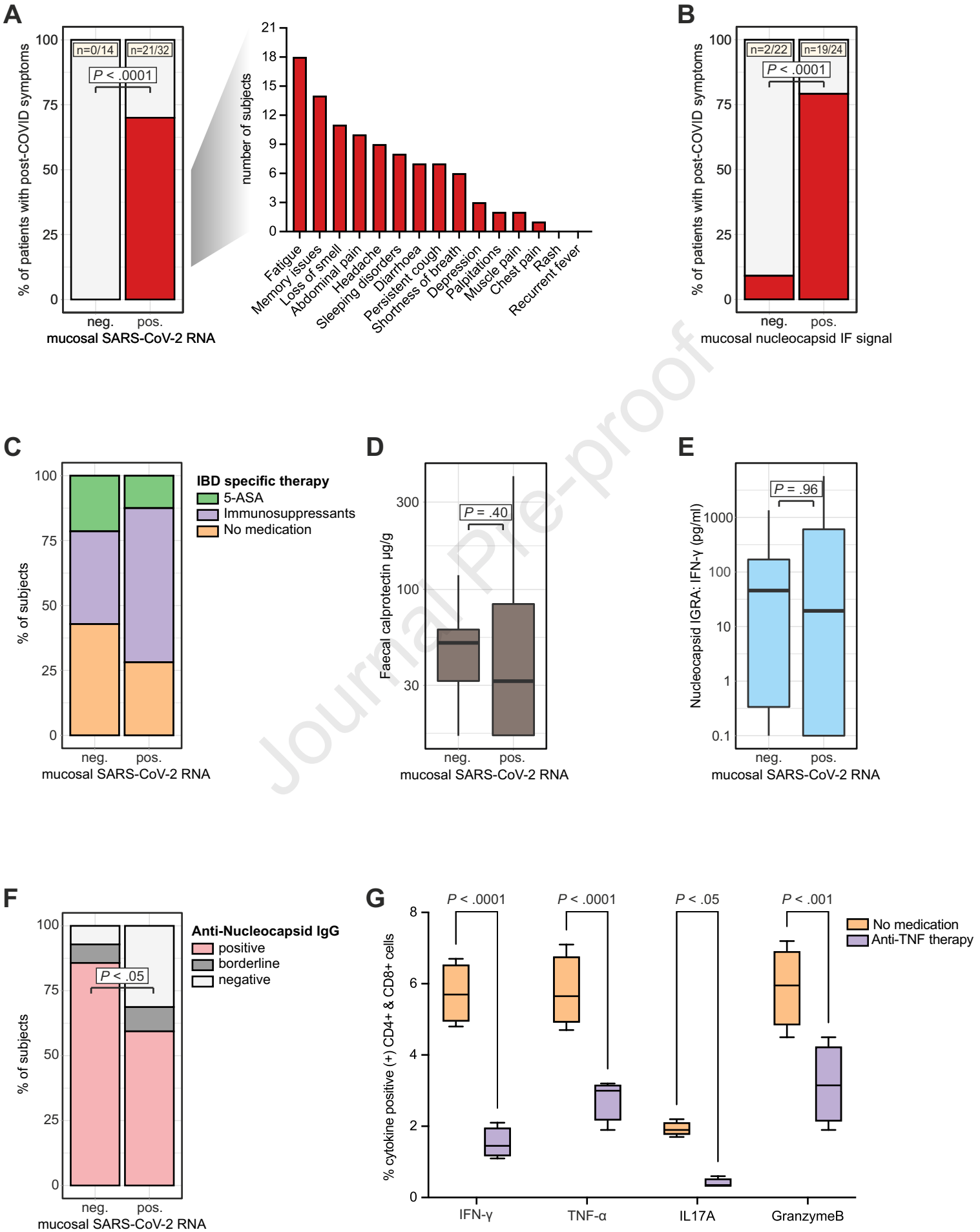

Supplementary

Supplementary Tables

Supplementary Table 1: SARS-CoV-2 and human qPCR primer pairs

Target gene	Forward Primer	Reverse Primer
SARS-CoV-2 genes		
Surface glycoprotein	GCTGGTGCTGCAGCTTATTA	AGGGTCAAGTGCACAGTCTA
Nucleocapsid phosphoprotein	CAATGCTGCAATCGTGCTAC	GTTGCGACTACGTGATGAGG
RNA-dependent RNA polymerase	AGAATAGAGCTCGCACCGTA	CTCCTCTAGTGGCGGCTATT
Envelope protein	TTCGGAAGAGACAGGTACGTTA	AGCAGTACGCACACAATCG
Human gene		
β-actin	CACCATTGGCAATGAGCGGTTC	AGGTCTTTGCGGATGTCCACGT

Primers were validated and extensively analysed by Park et al.[17]

Supplementary Table 2: General laboratory results of the study population

	Mucosal SARS-CoV-2 RNA negative	Mucosal SARS-CoV-2 RNA positive	Overall	p
n	14	32	46	
General laboratory parameters				
Urea (mg/dl)	24.05 [21.58, 25.53]	23.05 [18.00, 27.52]	23.90 [19.27, 27.40]	0.62
Creatinine (mg/dl)	0.81 [0.68, 0.91]	0.90 [0.75, 1.01]	0.86 [0.73, 0.97]	0.09
Total bilirubin (mg/dl)	0.74 [0.60, 1.08]	0.92 [0.55, 1.14]	0.86 [0.56, 1.13]	0.75
Sodium (mmol/l)	138.00 [137.00, 140.75]	139.00 [138.00, 140.00]	139.00 [138.00, 140.00]	0.40
Potassium (mmol/l)	3.70 [3.52, 4.02]	4.00 [3.70, 4.23]	3.90 [3.62, 4.20]	0.06
Chloride (mmol/l)	102.00 [101.25, 104.75]	103.00 [102.00, 105.00]	103.00 [102.00, 105.00]	0.49
ASAT (U/l)	21.50 [17.25, 32.25]	24.00 [19.75, 34.25]	22.50 [18.25, 34.75]	0.63
ALAT (U/l)	21.00 [13.25, 29.50]	23.50 [17.00, 41.00]	23.00 [17.00, 38.75]	0.31
Gamma GT (U/l)	16.50 [15.00, 28.75]	22.00 [15.75, 31.00]	20.00 [15.00, 31.25]	0.39
AP (U/l)	81.00 [65.75, 91.00]	78.50 [63.75, 92.00]	78.50 [64.25, 91.75]	0.83
LDH (U/l)	178.50 [164.75, 191.00]	190.00 [164.25, 201.50]	184.00 [164.25, 198.75]	0.53
CRP (U/l)	0.11 [0.06, 0.25]	0.10 [0.06, 0.21]	0.10 [0.06, 0.24]	0.76
Leukocytes (G/l)	6.00 [5.10, 6.27]	6.65 [5.22, 8.85]	6.25 [5.08, 8.45]	0.17
Erythrocytes (G/l)	4.69 [4.35, 4.94]	4.92 [4.49, 5.31]	4.86 [4.46, 5.18]	0.17
Haemoglobin (g/l)	136.00 [125.50, 145.50]	146.50 [138.75, 158.50]	144.50 [134.25, 153.00]	0.02
Haematocrit (%)	0.40 [0.38, 0.44]	0.44 [0.41, 0.46]	0.44 [0.40, 0.46]	0.02
MCH (pg)	28.80 [27.70, 31.40]	30.60 [29.25, 31.20]	30.25 [28.90, 31.20]	0.18
MCV (fl)	87.80 [82.55, 92.72]	89.40 [87.53, 92.70]	88.95 [85.95, 92.70]	0.36
MCHC (g/l)	331.00 [326.75, 339.75]	337.00 [328.00, 343.00]	336.50 [328.00, 343.00]	0.27
RDW (%)	12.95 [12.75, 13.60]	12.80 [12.47, 13.20]	12.90 [12.50, 13.20]	0.24
Thrombocytes (G/l)	242.00 [215.00, 297.25]	267.00 [223.75, 305.25]	262.50 [218.25, 302.75]	0.50
MPV (fl)	10.90 [10.27, 11.60]	10.65 [9.97, 11.10]	10.75 [10.00, 11.20]	0.25
Iron (µmol/l)	24.25 [18.52, 33.72]	25.85 [19.62, 32.75]	25.35 [19.28, 33.05]	0.80
Ferritin (µg/g)	73.00 [46.50, 172.50]	124.00 [73.75, 175.75]	118.50 [60.25, 174.75]	0.38
Transferrin (mg/dl)	269.50 [248.00, 295.50]	259.00 [236.75, 287.75]	261.50 [238.50, 289.25]	0.50
Transferrin saturation (%)	36.00 [28.75, 48.75]	37.00 [28.00, 53.00]	36.00 [28.00, 53.00]	0.96
Folate (µg/l)	8.85 [6.20, 13.30]	8.00 [6.90, 10.00]	8.00 [6.80, 10.30]	0.57
Vitamin B12	327.00 [308.75, 396.00]	293.00 [234.75, 353.75]	307.00 [237.75, 367.25]	0.15
Faecal calprotectin (µg/g)	51.45 [32.12, 60.48]	31.60 [16.00, 85.30]	36.95 [16.00, 69.88]	0.40

Data are reported as median with interquartile range in brackets

Supplementary Table 3: Antibodies for ICFC

Reactivity	Fluorochrome	Supplier	RRID
CD4	Pe	Biolegend	AB_1937247
CD8	PerCP	Biolegend	AB_1575072
CD45	BV785	Biolegend	AB_2563128
CD45RO	PeDazzle	Biolegend	AB_2566542
CD69	BV605	Biolegend	AB_2562306l
IFN-γ	BV421	Biolegend	AB_2561398
TNFα	APC	Biolegend	AB_315264
IL-17A	AF700	Biolegend	AB_2280255
GranzymeB	FITC	Biolegend	AB_2114575
Live/Dead	V510	Tonbo Biosciences	not available

ICFC= intracellular flow cytometry; IFN-γ= interferon gamma; TNFα= tumor necrosis factor alpha

Supplementary Figures

Supplementary Figure 1:

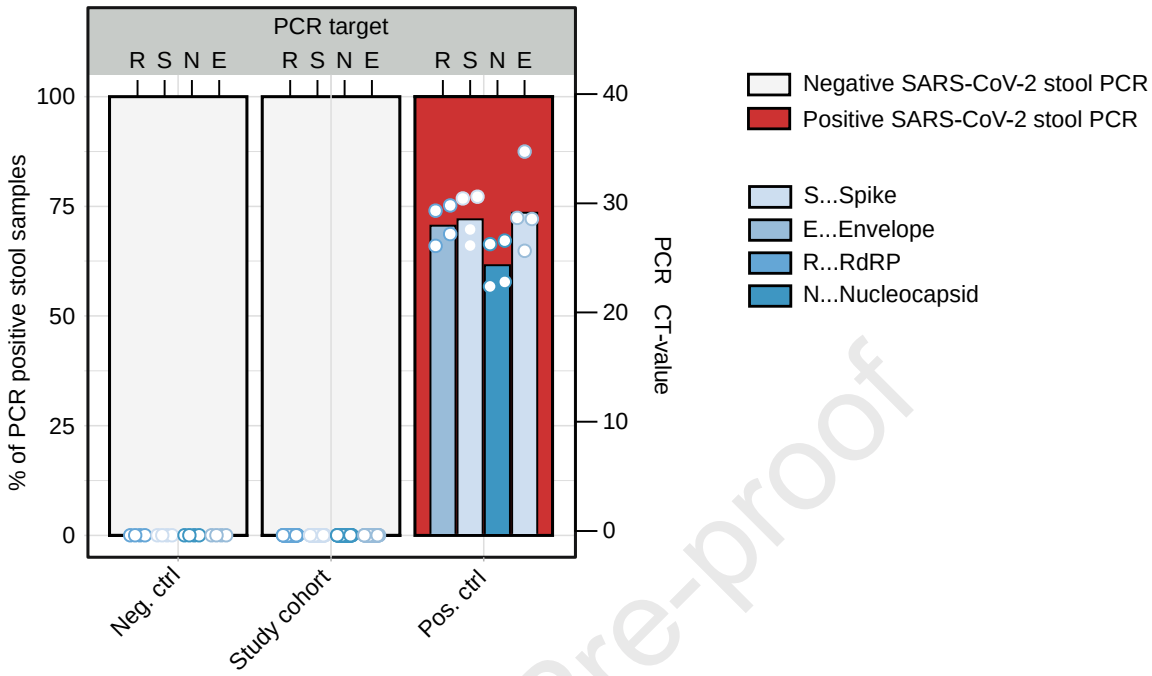

Supplementary Figure 1: Stool SARS-CoV-2 PCR. RNA was isolated from stool of patients before the pandemic (neg. ctrl; n=4), from the study cohort (n=46) and stool from COVID-19 subjects (pos. ctrl; n=4). The red bars indicate percentages of samples with positive SARS-CoV-2 PCR. The blue bars show CT-values for the RNA-dependent RNA polymerase (R), the spike (S), the nucleocapsid (N) and the envelope (E).

Supplementary Figure 2:

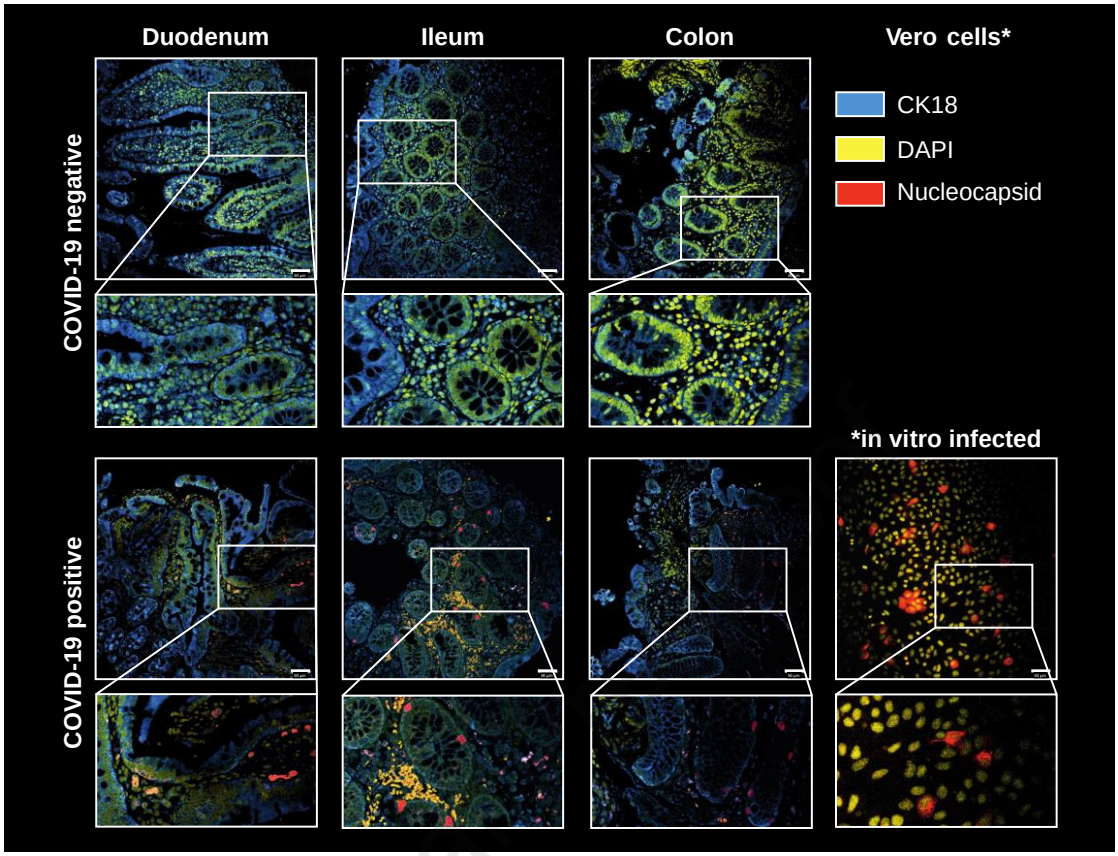

Supplementary Figure 2: SARS-CoV-2 nucleocapsid immunofluorescence of intestinal tissue. Representative confocal microscopy images of viral nucleocapsid (red) in the duodenum, ileum and colon mucosa from IBD patients ~219 days after acute COVID-19 (lower panel). Immunostaining of sections from patients with no history of SARS-CoV-2 infection (retrieved before the pandemic) is shown in the upper panel and serves as a negative control. Cytokeratin 18 (blue) visualises the cytoskeleton and DAPI (yellow) depict the nucleus. Scale bar indicates 50 µm.

Supplementary Figure 3:

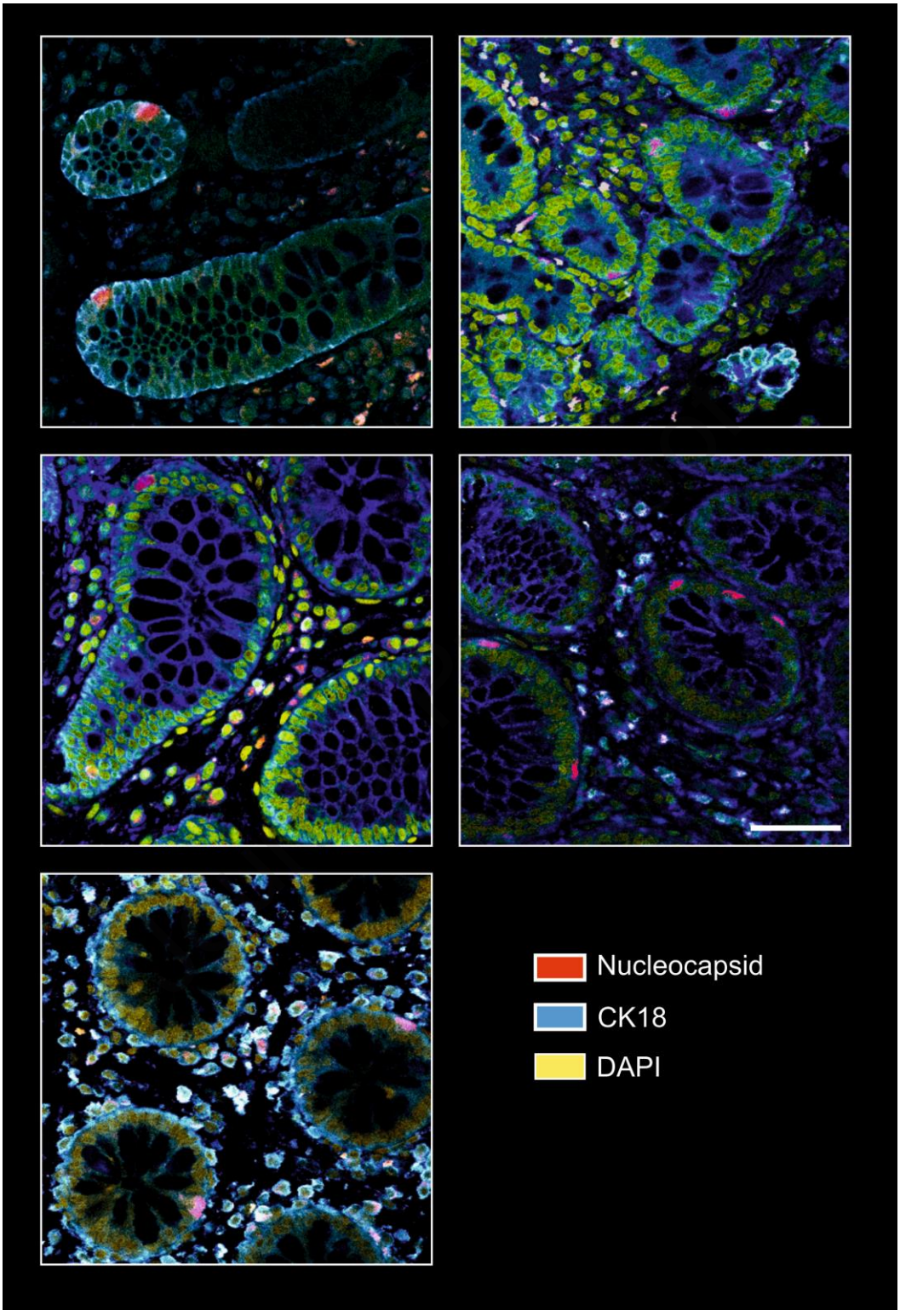

Supplementary Figure 3: Additional SARS-CoV-2 nucleocapsid immunofluorescence from intestinal tissue: As in Supplementary Figure 1: Representative confocal microscopy images of viral nucleocapsid (red) in the duodenum, ileum and colon mucosa from five IBD patients ~219 days after acute COVID-19. Cytokeratin 18 (blue) visualises the cytoskeleton and DAPI (yellow) depict the nucleus. Scale bar (bottom left) indicates 50 µm.

Supplementary Figure 4:

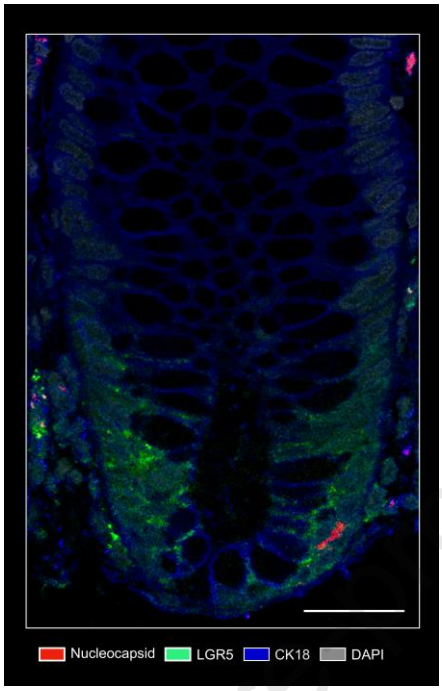

Supplementary Figure 4: Nucleocapsid/Lgr5 immunofluorescence: Representative confocal microscopy image of co-stainings of viral nucleocapsid (red) and Lgr5 (green) in the mucosa from an IBD patient ~219 days after acute COVID-19. Cytokeratin 18 (blue) visualises the cytoskeleton and DAPI (grey) depicts the nucleus. Scale bar indicates 100 µm.

Supplementary Figure 5:

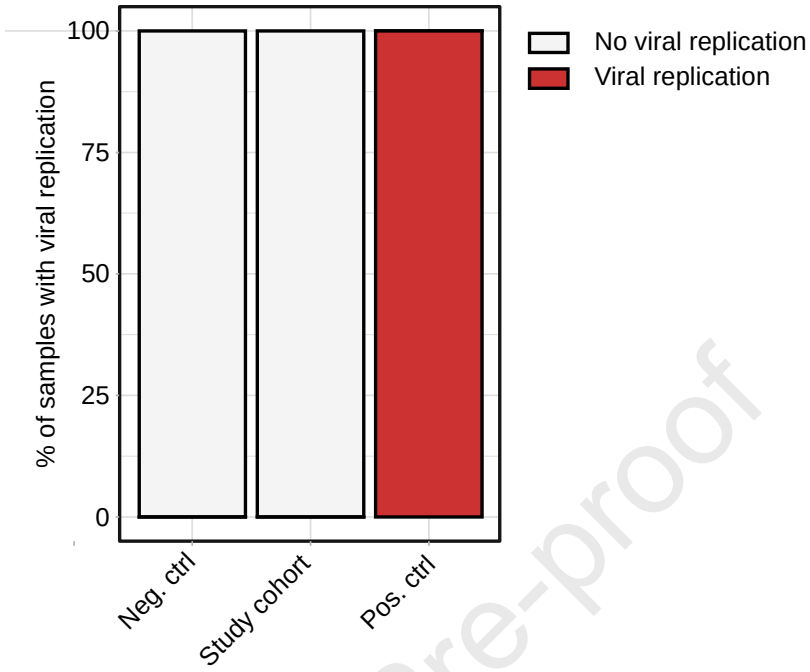

Supplementary Figure 5: SARS-CoV-2 cultivation: Lysates of negative controls (n=4), the study cohort (n=46) and positive controls (n=4) were used to infect ACE-2 and TMPRSS2 overexpressing Vero cells (Vero-TMPRSS2/ACE2) and cytopathic effect was analysed. The percentages of samples showing a cytopathic effect are indicated in red.

Supplementary Figure 6:

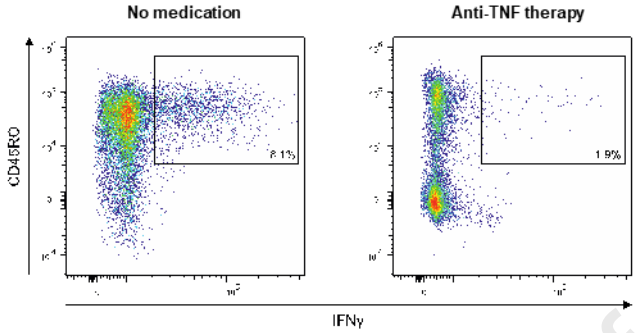

Supplementary Figure 6: Representative flow cytometry plots of cellular nucleocapsid reactivity. PBMCs were co-cultivated with peptide pools covering the N protein for 60 h, restimulated and analysed by intracellular cytokine staining. Dot plots show $CD4^+$ and $CD8^+$ T cells that produced IFN-γ in response to stimulation nucleocapsid peptides in an IBD patient without medication (left) and a patient with anti-tumor necrosis factor (TNF) therapy (right).

Supplementary Figure 7:

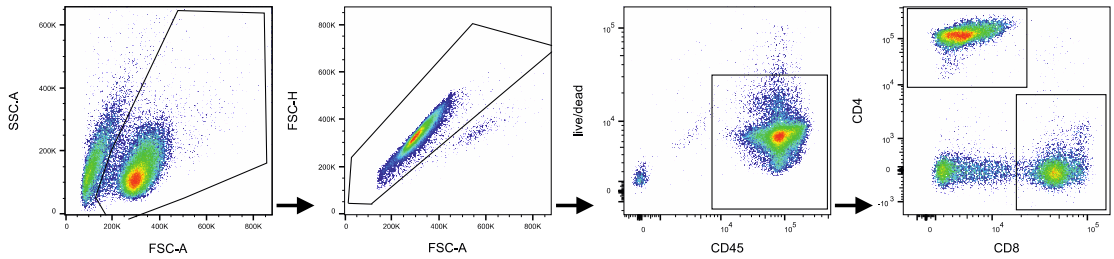

Supplementary Figure 7: Representative gating strategy. First cells were gated based on FSC and SSC; singlets were excluded by FSC-A vs. FSC-H gate; live CD45$^+$ high leukocytes were gated; live CD45+ high cells were separated in CD4$^+$ and CD8$^+$ cells. These cell populations were analysed for intracellular IFN-γ, TNFα, IL-17 and GranzymeB.

Supplementary Methods

Immunofluorescence

Intestinal biopsy specimens were collected in RPMI and immediately transferred in cryomolds, covered with OCT embedding medium and immersed in cold isopentane with liquid nitrogen until snap-frozen. Cryomolds were stored at -20°C until cryosectioning. For downstream immunofluorescence four µm cryostat sections were cut from the samples and subsequently stained for SARS-CoV-2 nucleocapsid and epithelial CK18. according to a standardized immunofluorescence protocol. In brief endogenous peroxidase was blocked using Dako peroxidase block (Agilent, CA, USA). Slides were incubated with Image-iT FX signal Enhancer (#I36933Thermo Scientific, Massachusetts, US) and subsequently stained using anti-nucleocapsid (#PA5114448, Thermo Scientific, Massachusetts, US), anti-CD8 (#14-0008-80, Thermo Fisher Scientific, Waltham, MA), anti-LGR5 (#MA5-25644, Thermo Fisher Scientific, Waltham, MA) and anti-CK18 (#LS-B11232, LifeSpan Biosciences, WA, US) antibodies. Targets were visualized with secondary fluorophore conjugated antibodies. Nuclei were counterstained using ProLong Diamond antifade reagent with DAPI (Invitrogen, CA, USA); 200 µm × 200-µm images were acquired on a Zeiss Axioobserver Z1 in combination with a LSM700 confocal laser scanning system containing four lasers with 405, 488, 555, and 654 nanometre wavelengths (Zeiss, Oberkochen, Germany).

Virus cultivation

Biopsies stored in RPMI supplemented with 10% FCS at -80°C were homogenized using a Precellys® 24 Homogenisator (Bertin, Montigny-le-Bretonneux, France).

The isolation protocol as described below has been established using nasal swabs from symptomatic COVID-19 patients (manuscript in preparation).

After homogenisation, the lysate was sterile filtrated through spin-x columns (Corning Inc, NY, US) and used to infect ACE-2 and TMPRSS2 overexpressing Vero cells[18] (Vero-TMPRSS2/ACE2). The inoculum was added to the cells for 1 h at 37 °C, after which cells were washed once and maintained in high glucose Dulbecco's Modified Eagle Medium (Merck, Darmstadt, Germany) supplemented with 2% FCS, 2% L-Glutamin, and 1% Penicillin-Streptomycin. Three days after infection, wells were analysed for cytopathic effect (CPE). For wells with clear CPE, virus was harvested and frozen in aliquots at -80°C. For wells with absent or only partial CPE, a second passage was performed. Fresh confluent Vero-TMPRSS2/ACE2 cells were infected for 1 hour with supernatant from the first passage. Subsequently, cells were washed and cultured for 3 days in complete medium with 2% FCS. Samples with absent CPE after two passages were regarded negative for infectious virus. All work with live SARS-CoV-2 was performed in biosafety laboratory level 3 facility.

Interferon gamma release assay (IGRA)

The presence of SARS-CoV-2 specific T cells directed against the spike (S) and nucleocapsid (N) proteins were assessed by interferon gamma release assays (IGRA) and validated with intracellular flow cytometry.[19] To specifically stimulate SARS-CoV-2 specific T cells, lithium heparin whole blood or isolated peripheral blood mononuclear cells (PBMC), were co-incubated with peptide pools (Miltenyi Biotech, Bergisch-Gladbach, Germany) consisting of 15-mer peptides with 11 amino acids overlap covering the entire sequence of the spike glycoprotein (pepS) and the complete sequence of the nucleocapsid phosphoprotein (pepN).

For the IGRA 600 µl lithium heparin aliquots whole blood were co-incubated with and without SARS-CoV-2 specific peptides. Four sample preparations were used to determine interferon-gamma (IFN-γ). One sample was mock treated to determine the steady state IFN-γ expression, in the second and third sample IFN-γ expressions were analysed upon stimulation with spike or nucleocapsid peptides (PepTivator SARS-CoV-2 ProtS, S1, S+ & N, Miltenyi, Bergisch Gladbach, Germany). An additional sample stimulated with PMA/Ionomycin served as a positive control. After 24 hours on 37°C, the samples were spun down at 2000 x g for 15 minutes and the supernatant was stored at -80°C. Concentrations of IFN-γ were measured using a human IFN-γ ELISA kit (BD OptEIA Set Human IFNg, BD Biosciences Pharmingen, New Jersey, US) according to the manufacturer's instructions. Negative control samples were diluted 1:5. SARS-CoV-2 peptide (pepS and pepN) co-incubated samples were diluted 1:5, 1:10, and 1:15. PMA stimulated samples were diluted 1:80 using dilution buffer. Spike and nucleocapsid reactivity were calculated by subtracting the untreated response from that of the stimulation

Intracellular flow cytometry

To decipher subsets of the T cell compartment, SARS-CoV-2 specific T cells were expanded and analysed by intracellular flow cytometry (ICFC). First lithium heparin whole blood was collected and PBMCs were isolated using a Lymphoprep density gradient medium (Stemcell, Vancouver, Canada) according to the manufacturer's instructions. In brief 4 ml lithium heparin blood were diluted with 3 ml PBS, PBMCs were isolated by layering the 7ml on 4 ml Lymphoprep and subsequent density-gradient centrifugation for 30 minutes at 850 x g. PBMCs were collected from the interphase, washed twice, cryopreserved in heat- inactivated FCS supplemented with 10% dimethylsulfoxid (Sigma, Missouri, US) and stored in liquid nitrogen until further use.

To expand SARS-CoV-2 reactive T cells, 2 × 10^5 PBMCs in 200 µl of RPMI medium supplemented with 10% FCS were pulsed with 0.6 µg/ml spike (pepS, pepS1 and pepS+) or nucleocapsid (pepN) peptide pools in the presence of 10 U/ml interleukine-2 (IL-2). Cells were cultured with IL-2 only served as a negative control. After 60 hours, cells were restimulated

with or without 1 µg/ml spike or nucleocapsid peptide pools. Cells stimulated with 4 µg/ml PHA served as positive controls. After combined surface (CD45, CD4, CD8, CD45RO, CD69) and intracellular cytokine staining (IFN-γ, TNFα, IL-17A, granzymeB) specific T cell responses were acquired on a CytoFLEX Flow Cytometer (Beckman Coulter, California, US) and analysed with Flowjo v10.6 (Becton Dickinson, New Jersey, US). As in IGRA spike and nucleocapsid reactivity was calculated by subtracting the untreated response from that of stimulation. A representative gating strategy is shown in Supplementary Figure 5. Antibodies and the respective suppliers are depicted in Supplementary Table 3.

What you need to know

Background and context

Long-term sequelae of coronavirus disease 2019 (COVID-19), collectively termed the post-acute COVID-19 syndrome, reflects a significantly growing health care challenge. To date, the pathophysiology of this debilitating multi-organ disease is poorly understood. We investigated whether severe acute respiratory syndrome coronavirus 2 (SARS-CoV-2) antigen persistence underlies the post-acute COVID-19 syndrome.

New findings

We report that SARS-CoV-2 antigens persist in the gut mucosa for months after acute COVID-19 in the majority of patients with IBD irrespective of immunosuppressive therapy or gut inflammation. Viral antigen persistence associates with post-acute COVID-19 symptoms.

Limitations

The concept of viral antigen persistence as driver of immune perturbation and post-acute COVID-19 syndrome should be corroborated in controlled clinical trials beyond IBD.

Impact

Collectively, our findings suggest that viral antigen persistence is a basis for post-acute sequelae of COVID-19, a rapidly emerging disorder across the globe.

Lay summary

Post-acute COVID-19 is a rapidly growing health care challenge across the globe. This study identifies that post-acute COVID-19 is accompanied by viral antigen persistence in the gut from patients with inflammatory bowel diseases.